



Sensors **2011**, *11*(1 1) , 10798-10819; [Open Access](#)
doi:[10.3390/s111110798](https://doi.org/10.3390/s111110798)

Article

Brillouin Corrosion Expansion Sensors for Steel Reinforced Concrete Structures Using a Fiber Optic Coil Winding Method

Xuefeng Zhao ^{1,*} ✉, **Peng Gong** ¹ ✉, **Guofu Qiao** ² ✉,
Jie Lu ¹ ✉, **Xingjun Lv** ¹ ✉ and **Jinping Ou** ^{1,2} ✉

¹ School of Civil Engineering, Dalian University of Technology, Dalian 116024, China

² School of Civil Engineering, Harbin Institute of Technology, Harbin 150090, China

* Author to whom correspondence should be addressed.

Received: 8 October 2011; in revised form: 10 November 2011 / Accepted: 12 November 2011 / Published: 16 November 2011

Abstract: In this paper, a novel kind of method to monitor corrosion expansion of steel rebars in steel reinforced concrete structures named fiber optic coil winding method is proposed, discussed and tested. It is based on the fiber optical Brillouin sensing technique. Firstly, a strain calibration experiment is designed and conducted to obtain the strain coefficient of single mode fiber optics. Results have shown that there is a good linear relationship between Brillouin frequency and applied strain. Then, three kinds of novel fiber optical Brillouin corrosion expansion sensors with different fiber optic coil winding packaging schemes are designed. Sensors were embedded into concrete specimens to monitor expansion strain caused by steel rebar corrosion, and their performance was studied in a designed electrochemical corrosion acceleration experiment. Experimental results have shown that expansion strain along the fiber optic coil winding area can be detected and measured by the three kinds of sensors with different measurement range during development the corrosion. With the assumption of uniform corrosion, diameters of corrosion steel rebars were obtained using calculated average strains. A maximum expansion strain of 6,738 $\mu\text{m/m}$ was monitored. Furthermore, the uniform corrosion analysis model was established and the evaluation formula to evaluate mass loss rate of

steel rebar under a given corrosion rust expansion rate was derived. The research has shown that three kinds of Brillouin sensors can be used to monitor the steel rebar corrosion expansion of reinforced concrete structures with good sensitivity, accuracy and monitoring range, and can be applied to monitor different levels of corrosion. By means of this kind of monitoring technique, quantitative corrosion expansion monitoring can be carried out, with the virtues of long durability, real-time monitoring and quasi-distribution monitoring.

Keywords: fiber optic; Brillouin sensor; corrosion sensor; fiber optic coil; steel reinforced concrete structure; structural health monitoring

1. Introduction

Steel corrosion has become a major problem worldwide, especially for structures exposed to aggressive environments. This problem has reached alarming proportions in the past three decades, leading to very high repair costs, sometimes even above the initial construction cost, or in extreme situations, to the final collapse of the structures [1–4]. **Figure 1** shows the schematic diagram of the corrosion process of the reinforcing steel rebar in concrete [5]. Concrete normally provides a high degree of protection to the reinforcing steel against corrosion, by virtue of the high alkalinity ($\text{pH} > 13.5$) of the pore

solution. Under high alkalinity, steel rebar remains passivated. However, when sufficient chloride ions (from de-icing salts or from seawater) have penetrated to the steel rebar in concrete or as the pH value of the pore solution drops to low values due to the carbonation process, the protective film on the steel rebar surface is destroyed and the reinforcing steel is depassivated. Corrosion in the form of rust formation and loss in cross-section of the rebar in the presence of oxygen and water (humidity) then occur. The corrosion of steel in concrete is essentially an electrochemical process [6–8].

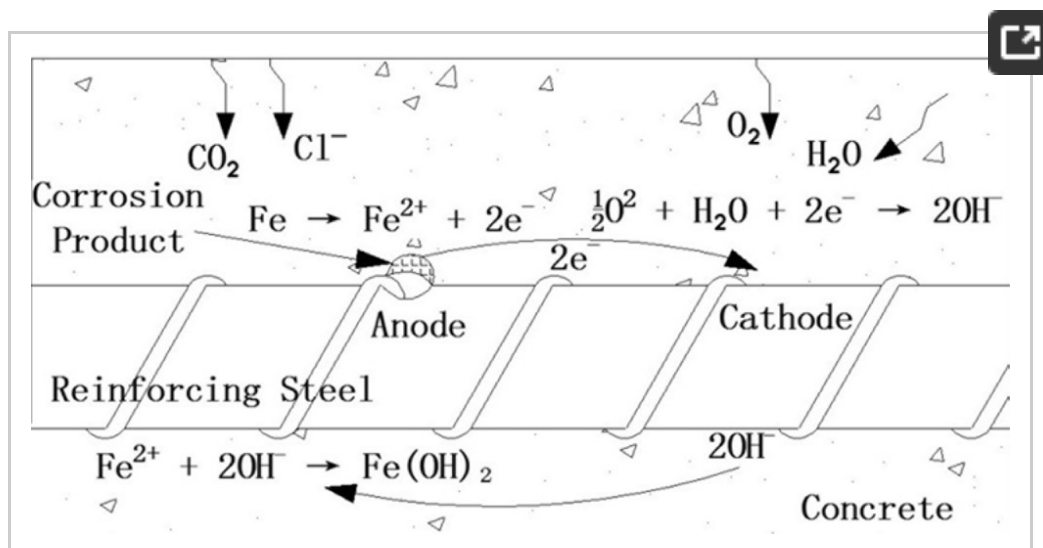


Figure 1. Schematic diagram of reinforcing steel corrosion in concrete as an electrochemical process.

Although the corrosion mechanics of the reinforcing steel are well-known, finding out the corrosion status of the structure in service is very urgent in practical engineering structures. Over the past two decades, structural health monitoring (SHM) has gained

worldwide acceptance as an economical way to obtain real-time data on the health, and subsequently the safety and serviceability of infrastructure systems [9]. Corrosion monitoring can provide much valuable information to SHM, the accurate monitoring of corrosion status of the steel rebar embedded in concrete in service life has been a technical challenge for a long time [10].

Recently, kinds of novel corrosion sensors have been applied in the health monitoring of large-scale civil structures such as buildings, dams, tunnels, river levees and other structures [11–13]. Among them, the fiber optical corrosion sensors are currently attracting considerable research interest in SHM owing to their distributed sensing ability, long sensing distance, high sensitivity, good durability, immunity to electromagnetic interference and other advantages [14,15]. Fuhr and Huston developed the fiber optical chloride detector, whose sensing mechanism relies on spectroscopic analysis of a chemical reaction of chloride and reagents [16]. Bennett designed a prototype optical fiber sensor for monitoring corrosion on large steel structures where the sensor works by pulling a multimode fiber into a tight bend and securing it with a “corrosion fuse” [17]. Li proposed a Fiber Optic Corrosion Sensor (FOCS) fabricated by electroplating a Fe-C alloy film onto an optical fiber core within the sensing region [18]. The research mentioned above needs extra packaging structures or sensing materials to transfer corrosion related parameters to fiber optic and make sensitive

parameters detectable, which will inevitably affect durability and stability of corrosion sensors.

Distributed fiber optical Brillouin sensing is a cutting-edge technique in the field of structural health monitoring for infrastructures. Because of its advantages, such as distributed measurement ability, corrosion resistance, good durability, *etc.*, it has become a hot field of scientific research around the world. In recent years, its widespread applications in field works have made important contributions to the safe operation of structures. The Brillouin Optical Time Domain Reflectometer/Analyser (BOTDR/A), which is based on the propagation of a train of incident pulses and Brillouin back-scattering that occurs when light is transmitted through an optical fiber [19–22], can conduct continuous monitoring of the temperature and strain distributed over long distances [23,24]. The successful applications in different areas show that fiber optical Brillouin sensing technique offers a bright prospect owing to its distinct capability to monitor temperature and strain distribution along the sensing fiber optic [25].

Because of the long durability and electromagnetic interference immunity of the optical Brillouin sensing technique, the development fiber optical Brillouin corrosion sensors would be promising if proper sensing packaging methods can be found. The distributed strain sensing ability offers the opportunity to use the fiber optic coil winding method to directly measure the expansion strain caused by corrosion. The sensing packaging structure

will be simple and no extra sensing materials and no complex packaging structure is needed. Based on fiber optical Brillouin technique, we propose a novel kind of fiber optic coil winding method to monitor the steel rebar corrosion expansion in reinforced concrete structures. Three kinds of novel Brillouin corrosion expansion sensors were designed and tested in this paper, in order to monitor corrosion development during long term service life of steel reinforced concrete structures.

2. Basic Principle of the Fiber Optical Brillouin Sensing Technique

The fiber optical Brillouin sensing technique is based on the Brillouin scattering phenomena. Fiber optics are utilized both as sensing elements and signal transmission media. When a short light pulse is launched into and transmitted along the fiber, the frequency of the Brillouin backscattering light can be measured at the same end. The time interval between sending the pulse and arrival of the backscattered light provides the spatial information, while the frequency of the backscattering light provides information of the temperature or strain distributed along the fiber optic. The backscattered Brillouin frequency is shifted from the incident light frequency because of the temperature variation and strain variation along the optic fiber. The Brillouin frequency shift is determined by the following equation:

$$f_B = 2nv_a / \quad (2.1)$$

where f_B is Brillouin frequency shift, n is refractive index of fiber, v_a is the acoustic wave velocity and λ is wavelength of incident light.

The relationship between the Brillouin frequency shift at a certain location along the fiber and its corresponding temperature and strain change can be described as the following equation:

$$f_B = k_f \epsilon + k_{ft} \Delta T + C \quad (2.2)$$

where ΔT is temperature change, k_{ft} is temperature coefficient, k_f is strain coefficient of Brillouin frequency shift, ϵ is strain change and C is a constant.

In the case of pure strain variations, there will be no temperature variations, so the relation can be simplified as:

$$f_B = k_f \epsilon + C \quad (2.3)$$

As a result, by measuring the Brillouin frequency shift we have access to the local temperature and strain conditions along the fiber optic.

3. Experiments

3.1. Strain Calibration Experiment

Single mode fiber optics with sensing lengths of 1 m and 2 m were studied, and strain calibration experiments were designed and conducted to obtain the strain coefficients for monitoring corrosion expansion strain. In the experiments, a steel tube with 5 cm of diameter was used to support fiber optics with sensing lengths of 1 m or 2 m, respectively, as [Figure 2](#)

shows.

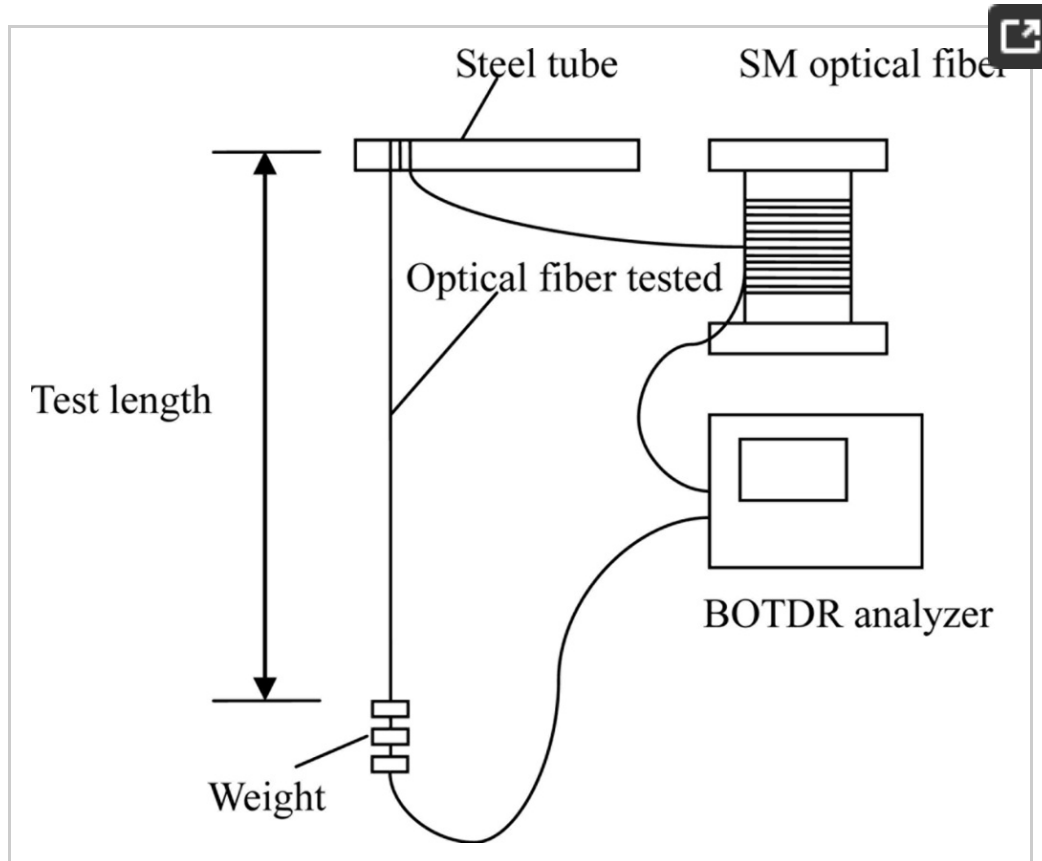


Figure 2. Setup of the strain calibration experiments.

Weight was loaded and unloaded using weights ranging from 0 to 200 g, in increments of 50 g. Two load cycles were conducted for each kind of test length. Spatial resolution of 1 m, and a sampling interval of 0.41 m was used for every experiment. The Brillouin frequency was measured using BOTDA analyzer in every load step.

Diameter of fiber optic is 0.125 mm, and Young's modulus is $0.72 \times 10^5 \text{ N/mm}^2$. According to elastic theory, there should be uniform strain distribution along the test length of fiber. When the weight of 50 g is loaded at the end of fiber, the strain change along

3.2. Design Principle of Brillouin Corrosion Expansion Sensors

When corrosion happens, the volume of the steel rebar will increasingly expand due to the rust product accumulation on the surface of the steel rebar. Rust depth is reported as two to six times of the volume of steel lost during the corrosion process [1,2], as shown in [Figure 3](#).

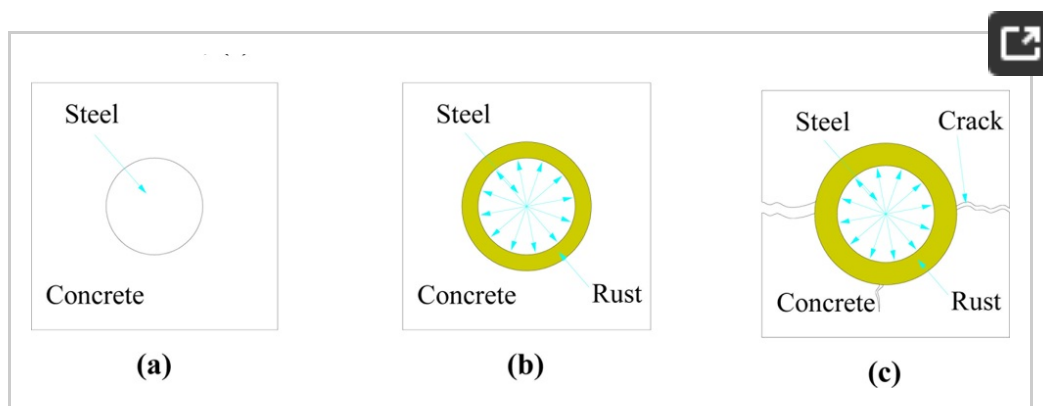


Figure 3. The corrosion process in the reinforced concrete; **(a)** without corrosion; **(b)** little amount of corrosion; **(c)** corrosion made concrete broken.

Therefore, we wind the single mode fiber optic around the polished steel rebar into a fiber optic coil, with a little pretension, as [Figure 4](#) shows. Then the fiber optic will be stretched when the volume of the steel rebar expands due to corrosion. Meanwhile, the tension strain change of the fiber optic coil in corrosion area can be monitored using the BOTDR/A analyzer, thus the corrosion process in the steel reinforced concrete structure can be monitored. Three

kinds of Brillouin corrosion expansion sensors: BCES-I, BCES-II, BCES-III, were designed based on this principle. Different detailed packaging schemes were proposed for the three kinds of sensors to test the sensitivity for corrosion expansion monitoring. The single mode fiber optic used is Corning G.657A/B, with a minimum bending curve radius of 7.5 mm, which will keep optical losses at a very low level after dozens of fiber optic coils are wound.

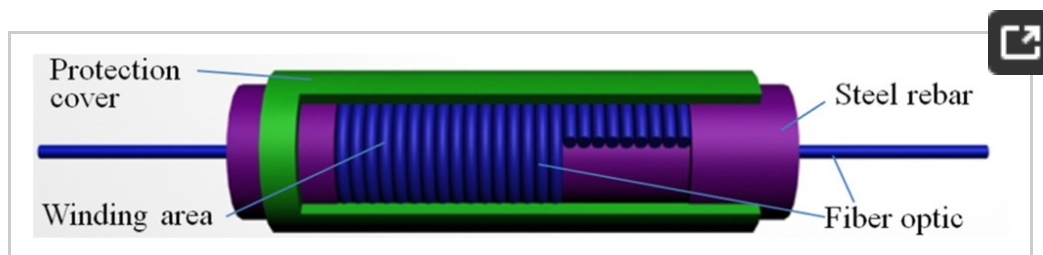


Figure 4. Basic packaging structure of the Brillouin corrosion expansion sensor.

3.3. Design of BCES-I

The design scheme of BCES-I is illustrated in [Figure 5](#) and the corresponding sensor packaging method follows the steps described below: (1) polish the surface of a 20 mm-length part of a steel rebar with diameter of 22 mm (■ 22), after which the diameter in polishing area decreased to 18.5 mm; (2) wind about 50 turns of single mode fiber optic into coils and guarantee the close contact of the fiber optic and steel rebar. The total winding length of the fiber optic is about 3.0 m; (3) fix both ends of the fiber on the rebar with epoxy glue, and draw out the fiber optic along the

steel rebar; (4) put one layer of porous soft material outside the optical fiber to prevent damage to the fiber optic coil winding; (5) add chain link fence outside the porous soft material layer to resist impacts and the vibration effects of casting concrete; (6) fix the chain link fence firmly on the deformed steel rebar with fine iron wire.

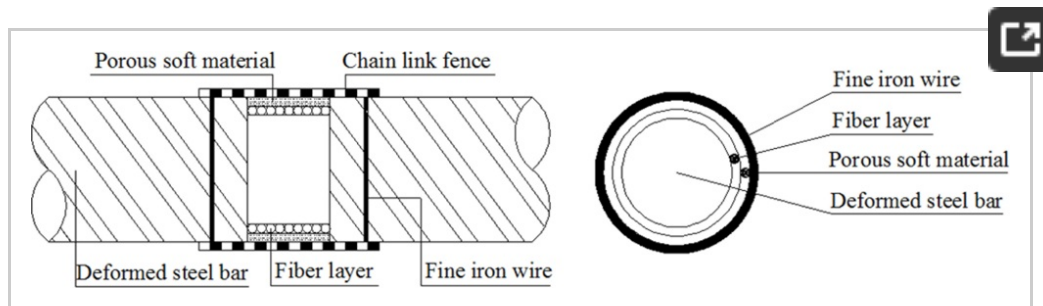


Figure 5. Packaging structure of BCES-I.

The single mode fiber optic was wound around the polished steel rebar directly. There was nothing between the fiber optic and corrosion rust; so any corrosion expansion caused by rust accumulation will be detected by the fiber optic coil winding. Porous soft material and chain link fence was not only used to protect the fiber optic, but also to make the penetration of chlorides more easier than with concrete material alone. The BCES-I sensor was designed to detect the steel rebar corrosion expansion at early stage.

3.4. Design of BCES-II

The design scheme of the BCES-II unit illustrated in [Figure 6](#) makes the following changes based on BCES-

I: (1) a porous soft material was added on the surface of the steel rebar and then waterproof lubricating film and fiber optic were wound; (2) the sensing optical fiber was coated with epoxy glue so that the optical fiber can deform in a coordinated fashion as a whole.

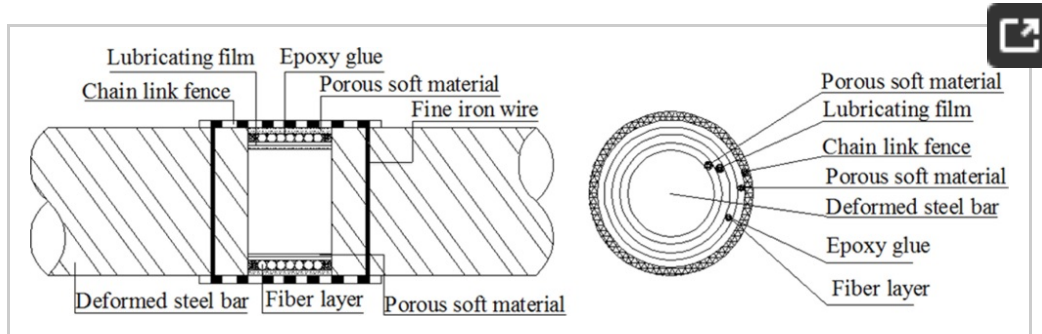


Figure 6. Packaging structure of BCES-II.

Single mode fiber optic was wound around the lubricating film layer. Corrosion expansion will act on the lubricating film layer first, and then on the fiber optic coil windings. Epoxy glue was used to provide better protection of the fiber optic. Because of the existence of lubricating film, the expansion strain along the winded fiber optic will be more even. Sensor BCES-II was designed to detect the steel rebar corrosion over a relatively big measurement range.

3.5. Design of BCES-III

The design scheme of BCES-III is illustrated in [Figure 7](#). It incorporates the following changes compared to BCES-I: (1) porous soft material was added on the polished steel rebar plus two polytetrafluoroethylene (PTFE) gaskets whose internal surfaces closely contact the porous material layer; (2) thin

lubricating film is wound on the PTFE gaskets, so as to minimize the stress accumulation generated in the contact area of the optical fiber and PTFE gaskets and thus guarantee compatible deformation of the sensing fiber after corrosion and expansion of the steel rebar; (3) the sensing fiber optic is wound around the lubricant film and the fiber coated with epoxy glue so that the fiber deforms uniformly as a whole.

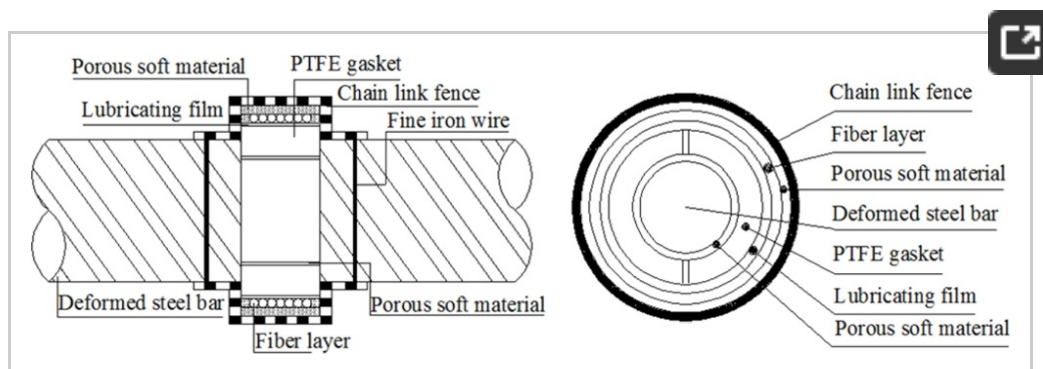


Figure 7. Packaging structure of BCES-III.

Single mode fiber optic was wound around the lubricating film layer on the outside of PTFE gaskets. Corrosion expansion will act successively on the porous soft material layer, PTFE gaskets, lubricating film layer and finally on fiber optic coil windings. The BCES-III sensor was designed to detect the steel rebar corrosion expansion over a relatively big measurement range.

3.6. Accelerating Corrosion Experiment System

In order to study the sensitivity of the developed Brillouin corrosion expansion sensors, an electrochemical corrosion acceleration experiment

system, shown in [Figure 8](#), was built to accelerate the steel rebar corrosion process in concrete specimens. In the system, the steel rebar was the anode and the stainless steel plate was the cathode. When electric current was applied, the circuit between the steel rebar and the plate was conducted by Cl^- , which will continuously transport Cl^- ions in the solution to the surface of the rebar. Cl^- is one of the most important factors influencing the corrosion of the steel rebar, and therefore this kind of experimental setup can accelerate the rate of corrosion enormously. During the experiment, the mass concentration of the solution of NaCl is 5.0%, and a constant voltage or constant current source was applied.

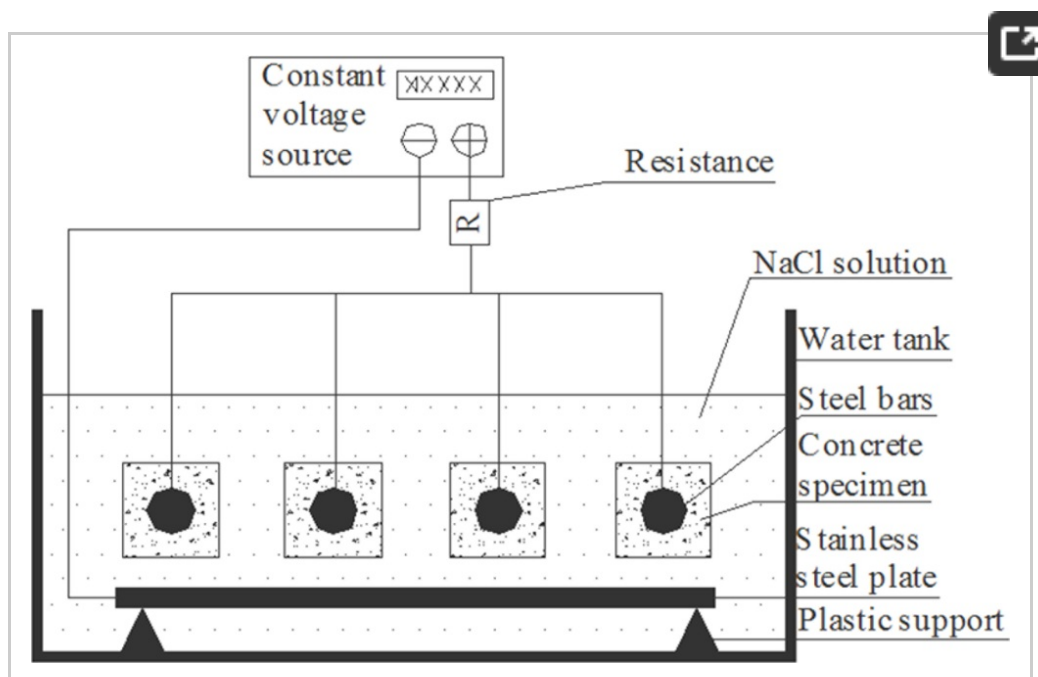


Figure 8. Schematic diagram of the electrochemical corrosion acceleration experiment system.

Before the experiment, the corrosion sensors were embedded into concrete specimens by concrete

casting, and concrete specimens with embedded BCES-I sensors [sensor names: S.1 (I), S.2 (I)] were numbered specimens No. 1 and No. 2, respectively. The specimen with BCES-II [sensor name: S.3 (II)] was numbered No. 3, and the specimen with BCES-III [sensor name: S.4 (III)] was numbered No.4, as shown in [Figure 9](#); the size of all concrete specimens was 100 mm × 100 mm × 300 mm. Concrete ultimate strength was 30 MPa. The cement used was P.O 32.5, and the concrete mass mix ratio was cement-water-sand-aggregate = 1:0.53:1.64:3.49. Only one sensor was embedded into each concrete specimen, placed along the axis of the specimen. After casting, the specimens were steam cured for 7 days, and then they were kept at room temperature at 22 °C for 3 days before they were tested.

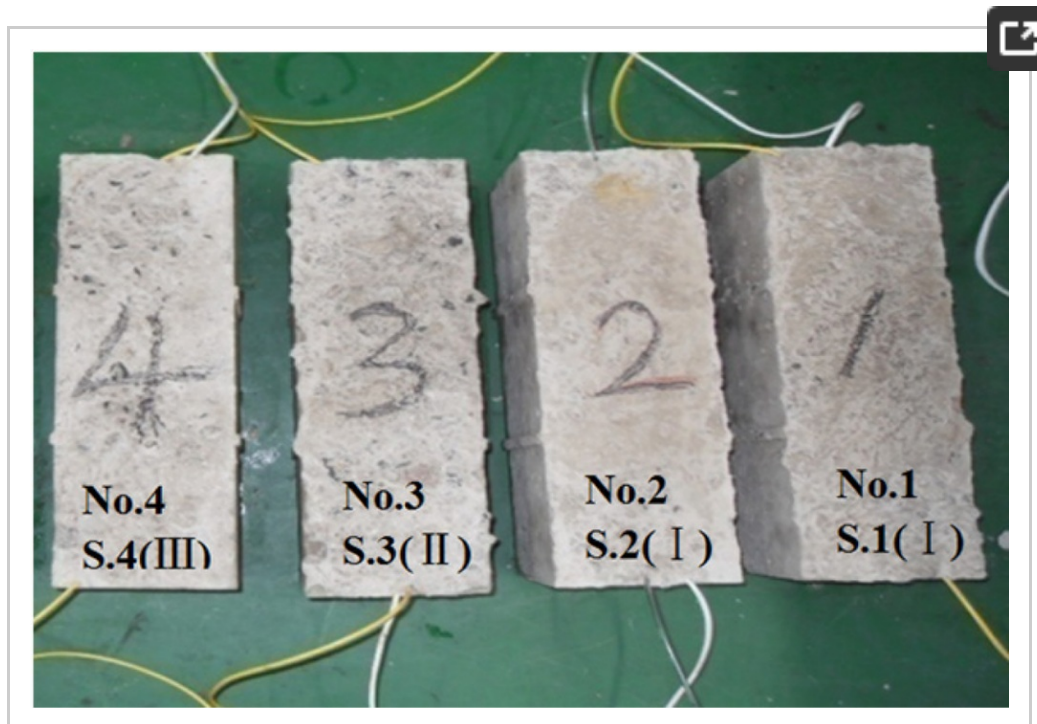


Figure 9. Concrete specimens with embedded sensors.

The BOTDA analyzer used in the experiments is a DiTest STA202-C instrument manufactured by the Omnisens Company. It was used to collect monitoring data during the experiments, whose sampling interval was 0.41 m, spatial resolution 1.0 m, and strain resolution is 2 $\mu\epsilon$. The BOTDA analyzer was set up to automatically scan the fiber optic circuit every one hour during the experiments.

The experiments were divided into two parts and the fiber optic circuit is shown in [Figure 10](#). Experiment one involved conducting the corrosion monitoring experiment of specimens No. 1 and No. 2. In the experiment, the fiber optics of S.1 (I) and S.2 (I) were connected together into one fiber optic circuit, and therefore quasi-distributed corrosion monitoring was conducted. A constant voltage source device was applied to supply electrical current. Voltage between the plate and the end of each specimen is 31.5 V. Experiment two was with specimens No. 3 and No. 4. Similarly, S.3 (II) and S.4 (III) were connected together into one fiber optic circuit. But in this case a constant current source was used, and the currents through the two specimens were 0.17 and 0.20 A, respectively.

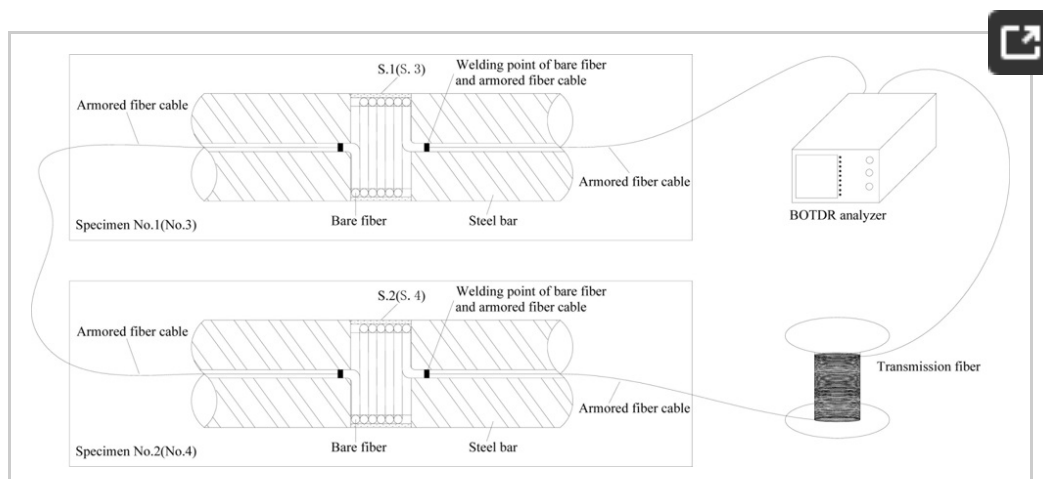


Figure 10. Fiber optic circuit of the corrosion monitoring experiments.

4. Experimental Results and Discussion

4.1. Strain Calibration Experiment

In the fiber optic circuit, only the sensing fiber optic with length of 1 m and 2 m is under extension load. There is signal change of the Brillouin frequency in the sensing fiber area, and no apparent signal change is found in any other part of fiber optic circuit, as [Figure 11](#) shows. The signal peak grows gradually as loads from 0 g to 200 g were added in increments of 50 g. The maximum value at each signal peak is used to calibrate the strain coefficient.

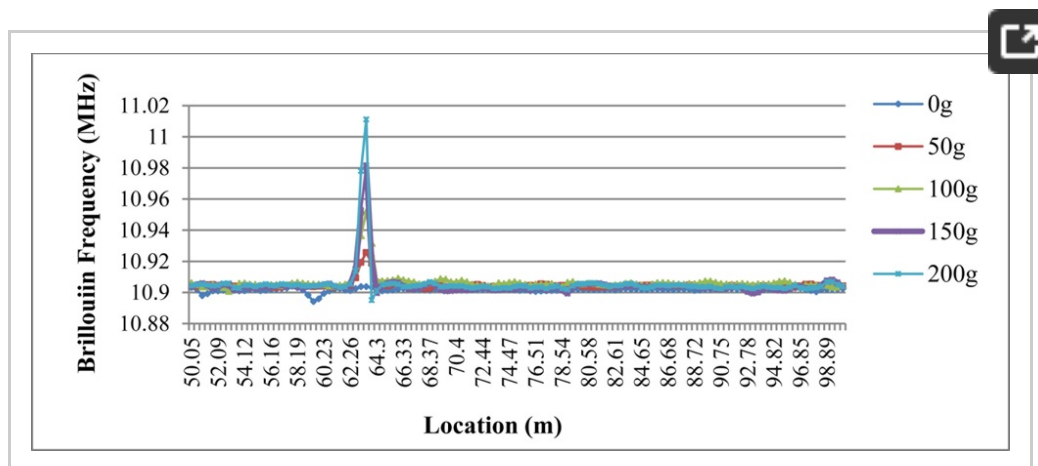


Figure 11. Brillouin frequency results of Load cycle 1 with sensing length of 1 m.

There were very good linear relationships between strain and Brillouin frequency, when the test lengths

are 1 m and 2 m, as [Figure 12](#) shows. Also, good linear relationships between strain loaded and Brillouin frequency are found. An average strain coefficient of 0.048 MHz/■■■■ was obtained.

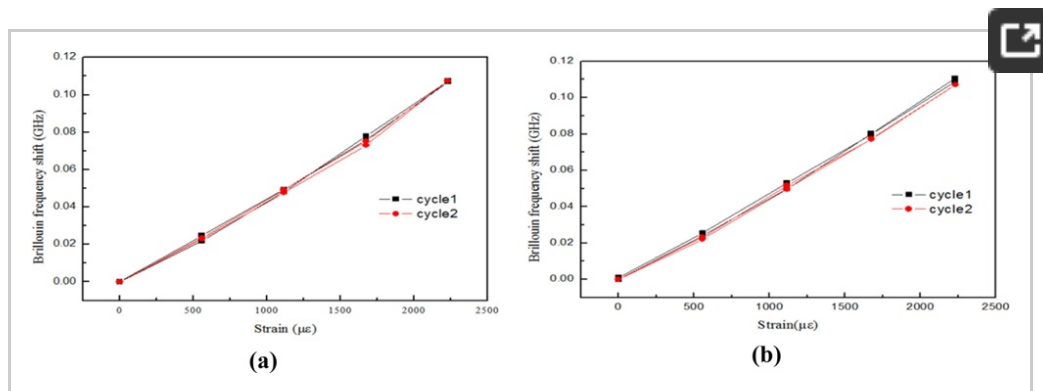


Figure 12. (a) Strain sensitivity result of sensor with length of 1 m; (b) Strain sensitivity result of sensor with length of 2 m.

The strain calibration experimental results show that single mode fiber optics with sensing lengths of 1 m and 2 m can serve as strain sensors. The strain coefficients obtained with the two kinds of length show very good agreement. There is very good linearity of the results with the BOTDA analyzer using the spatial resolution of 1 m and sampling interval of 0.41 m.

4.2. Result Analysis of BCES-I

The electrochemical corrosion acceleration experiment was conducted on the two specimens No. 1 and No. 2 continuously until the signal of sensing fiber of S.1 (I) became so weak that the BOTDA analyzer could not detect it. Experiment 1 lasted for 35

h. A large crack caused by corrosion was found on surface of specimen No. 1 after the experiment.

Figure 13 shows the relationship between distances, time and expansion strain measured by BOTDA analyzer.

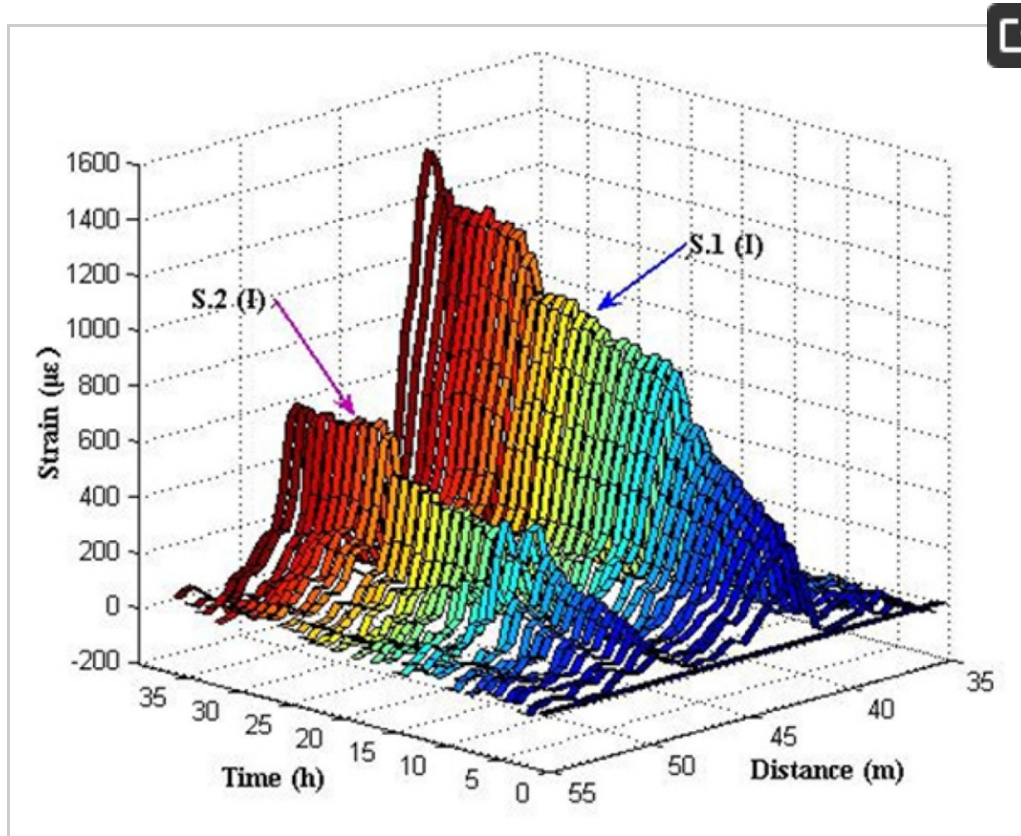


Figure 13. The expansion strain results of S.1 (I) and S.2 (I).

In Figure 13, there are two expansion strain peaks at the distance 41–42 m and 48–49 m, where the fiber optic coil windings of sensor S.1 (I) and S.2 (I) are located in the fiber optic circuit of the experimental system. Results reveal that S.1 (I) and S.2 (I) can monitor the strain distribution in the fiber optic coil winding area caused by the steel rebar corrosion expansion in the specimens. No apparent strain change was detected in other locations of the fiber

optic. Expansion strains increase steadily over time, which illustrates that the degree of corrosion grows gradually over time.

Furthermore, the average strains of the fiber optic coil windings of S.1 (I) and S.2 (I) and the straight-line fitting results were obtained, as shown in [Figure 14](#). Because the voltage and the mass concentration of NaCl solution were constant and ignoring the non-uniform distribution of Cl^- in the solution, steel corrosion expansion will increase linearly. In [Figure 14](#), the R^2 values (square of correlation coefficient) of the corresponding fitted lines were 0.935 and 0.945, respectively, which shows that the average strain curves had good linearity during the corrosion monitoring experiment. The BCES-I monitoring results perfectly reflect the increasing trend of the linear development of steel corrosion, which indicates that this kind of sensor can monitor the real progress of steel corrosion, effectively.

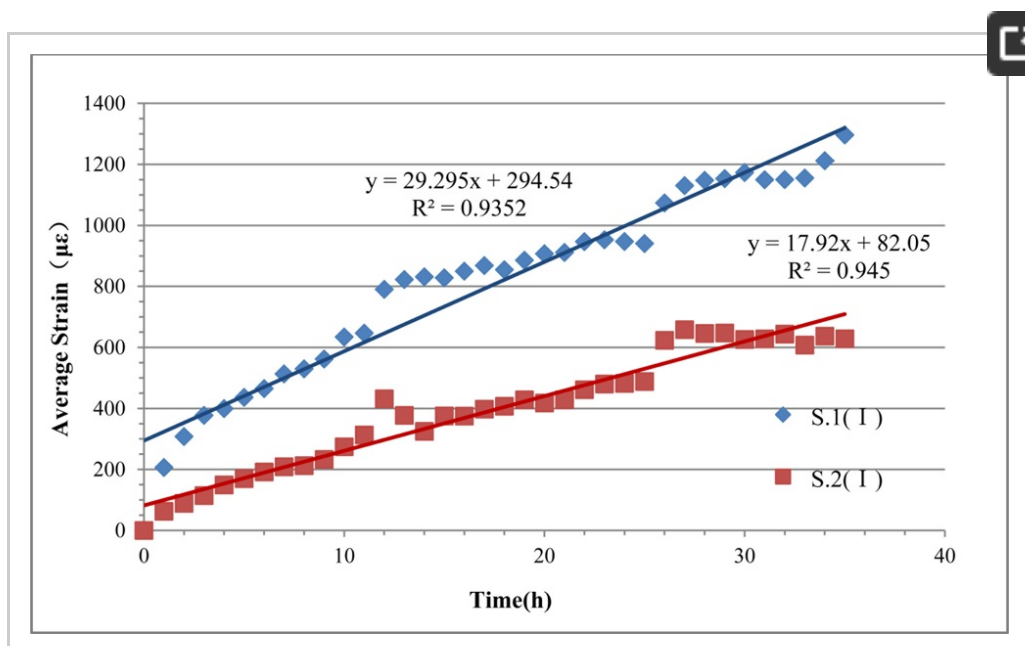


Figure 14. The average strains of sensor S.1 (I) and S.2 (I).

According to the electrochemical method theory, the current is directly related to the rate of corrosion of steel rebars. The resistance of concrete will change a little in the experiment, so if the voltage is constant, the current will change during the experiment, and then corrosion speed of steel bars will change a little accordingly. Theoretically, the fitted lines should go through the origin of coordinates, however, as can be seen in [Figure 14](#), neither of the fitted lines does, which is due to the reason that the unstable current under constant voltage in the initial phase brings about a surge in the steel corrosion rate. It can also be seen that average strains of sensing fibers in S.1 (I) and S.2 (I) increase over time, and the maximum strains reach 1,297 $\mu\epsilon$ and 658 $\mu\epsilon$, separately.

With the assumption of even corrosion during the experiment, there will be one layer of rust outside of the steel rebar with uniform thickness and also a linear relationship between circumference and diameter of the steel rebar with corrosion. The diameter of steel rebar with corrosion in sensor S.1 (I) and S.2 (I) can be calculated according to the average expansion strain result, as shown in [Figure 15](#). Results show that diameter of sensor S.1 (I) increases to 18.524 mm, with a 0.024 mm increment compared to its initial status. The diameter of sensor S.2 (I) increases to 18.512 mm, with a 0.012 mm increment.

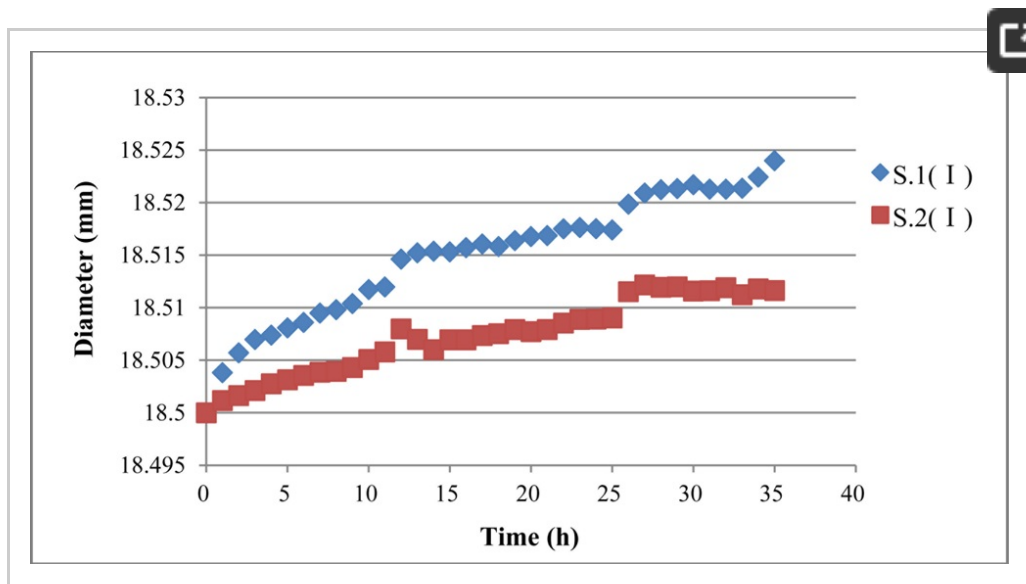


Figure 15. Steel rebar diameter monitored of sensor S.1 (I) and S.2 (I).

After the experiment, an obvious crack was found across three planes on the surface of specimen No.1, as [Figure 16](#) shows. The crack ran from the bottom to the side plane and its length reaches 68 mm at the side plane. For practical applications, in most cases a crack with this length would severely threaten the safety of the structure. After the experiment, no apparent crack appears on the surface of specimen No. 2. Crack observation results showed good agreement with the expansion strain and diameter results.

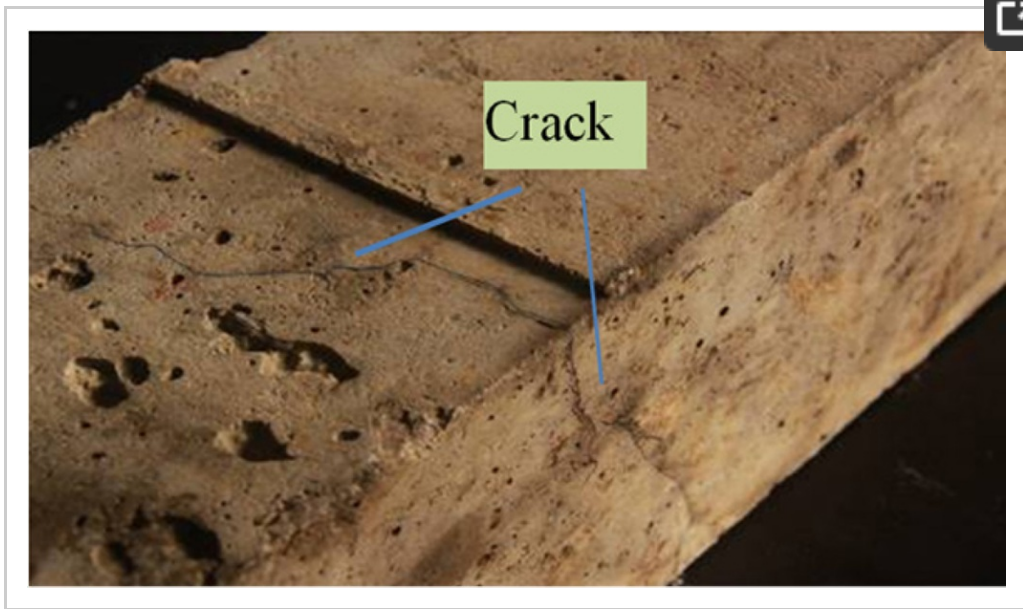


Figure 16. The crack on specimen No.1.

The steel corrosion in specimen No.1 and No.2 after experiment one is shown in [Figure 17](#). There is obvious corrosion rust distributed between the steel rebar and fiber optic coil windings.

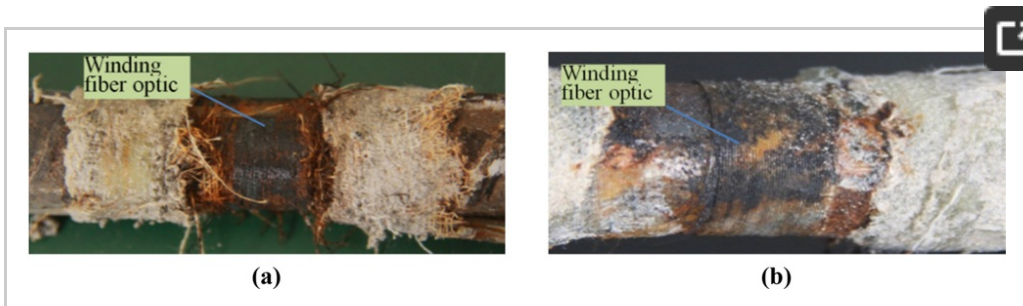


Figure 17. (a) The steel corrosion of S.1 (I) in the specimen No. 1; (b) The steel corrosion of S.2 (I) in the specimen No. 2.

Results of experiment one show that the advantages of BCES-I in the monitoring of steel rebar corrosion expansion can be summarized as follows:

1. The high sensitivity of BCES-I guarantees that the corrosion expansion strain of steel rebar can be monitored accurately and effectively. The corrosion signals were detected even within an hour after the experiment started, which reveals that early corrosion of steel rebars can be monitored effectively by this kind of sensor.
2. The steel corrosion expansion monitoring range of BCES-I is quite wide, from the beginning of corrosion to the appearance of large cracks in the specimen, which can satisfy the need of practical engineering applications.
3. BCES-I has good linearity and, it can carry out the real-time, quasi-distributed and quantitative steel corrosion monitoring.

The following disadvantages of BCES-I in the steel rebar corrosion expansion monitoring can be mentioned:

1. The sensing fiber optic coil winding of BCES-I has direct contact with the surface of the steel rebar, which leads to the fact that fiber optic is vulnerable when corrosion rust accumulates and large cracks of concrete appear; therefore, the sensor is not applicable to the condition of serious corrosion.
2. When the temperature varies greatly, the measured results are influenced a lot, and thus it is not applicable to environments with great variations of temperature, and some form of

temperature compensation technique should be considered in future work. The improvement plan of BCES-I is to develop temperature compensation so that it can be applied in a temperature-varying environment.

4.3. Results Analysis of BCES-II

Electrochemical corrosion accelerating experiment two was conducted on specimens No. 3 and No. 4 continuously until the signal of sensing fiber optic became so weak that the BOTDA analyzer cannot detect it. The experiment lasted for 502 h (more than 20 days), which resulted in serious corrosion of specimens. Large cracks were found in two specimens. [Figure 18](#) shows the relationship between distances, time and expansion strain of S.3 (II) measured by the BOTDA analyzer.

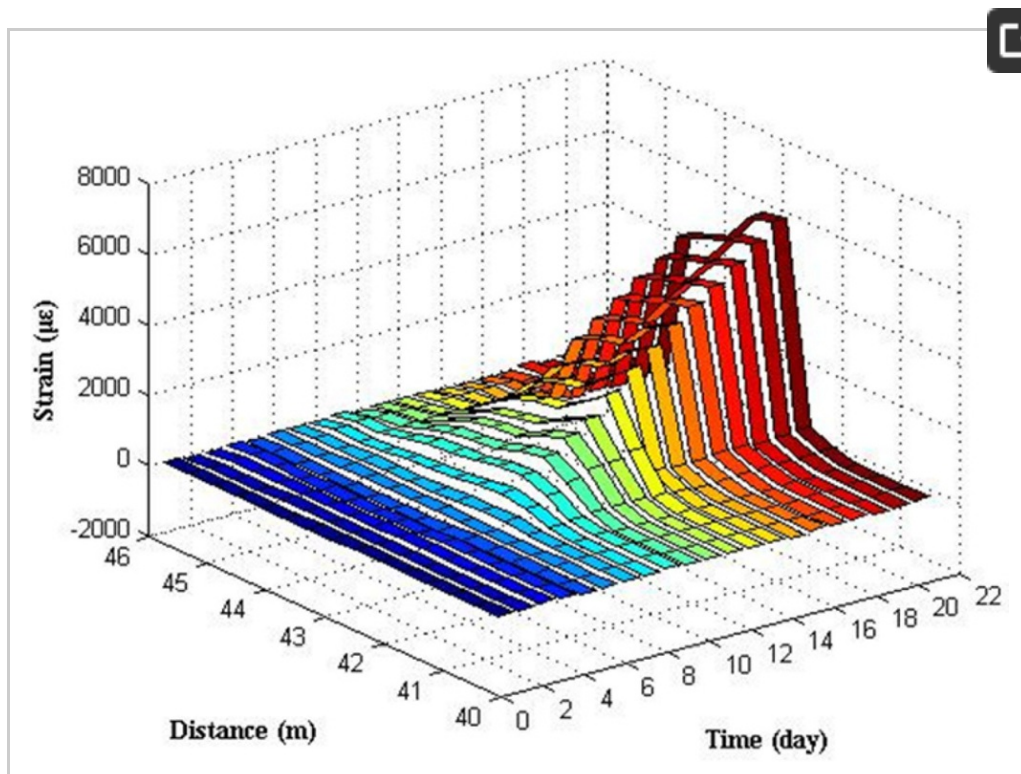


Figure 18. Corrosion expansion strain results of S.3 (II) in experiment two.

In [Figure 18](#), there clearly exists one strain peak in the fiber optic coil winding area, whose location in the fiber optic circuit is from 42.5 to 43.5 m. Result reveals that S.3 (II) can monitor the steel rebar corrosion expansion strain in the specimen. Because of the presence of a porous soft material layer and lubricating film between steel rebar surface and fiber optic coil winding, the expansion strain distribution along the sensing fiber became more even, and the peak became a little flat in comparison with BCES-I. No strain variation was measured along the fiber optic which is not located in the winding area. Expansion strain increased over time, which illustrates that the degree of corrosion grows gradually over time. Average expansion strain in the fiber optic coil winding area of S.3 (II) was calculated, as shown in [Figure 19](#).

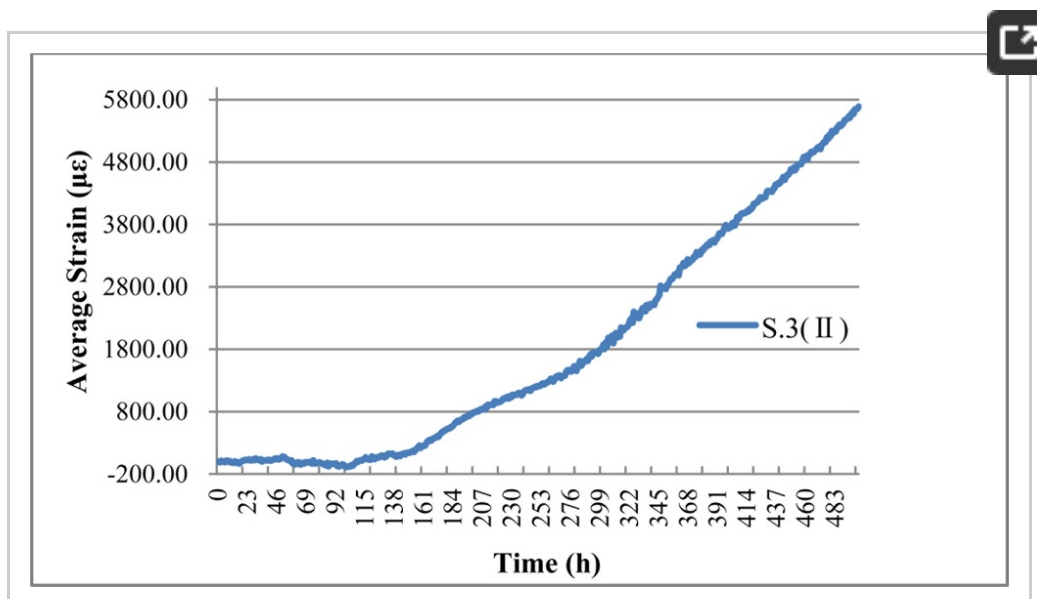


Figure 19. The average expansion strain result of S.3 (II).

There is an evident growing trend over time, which reaches the maximum strain of 5,690 $\mu\epsilon$ at the 502th hour. BCES-II expands the corrosion monitoring range to about four times more than BCES-I. The reason is mainly attributable to the soft porous material and lubricating film located between the steel rebar surface and the wound fiber optic, which isolates the sensing fiber from the surface of the steel rebar, and reduce the micro bending caused by corrosion rust accumulation. Simultaneously, a small space in the porous material and tiny gaps between packaging layers will reduce the sensitivity of BCES-II, as BCES-I only detected steel corrosion expansion after about 100 h, and then expansion strain increases linearly. The delay of corrosion expansion monitoring is also partially due to the epoxy glue's protection from corrosion.

With the assumption of even corrosion during the experiment, the diameter of the steel rebar in sensor S.3 (II) was calculated according to the average strain result, as shown in [Figure 20](#). Results show that the diameter of sensor S.3 (II) increases to 18.605 mm, with a 0.105 mm increment over the initial status.

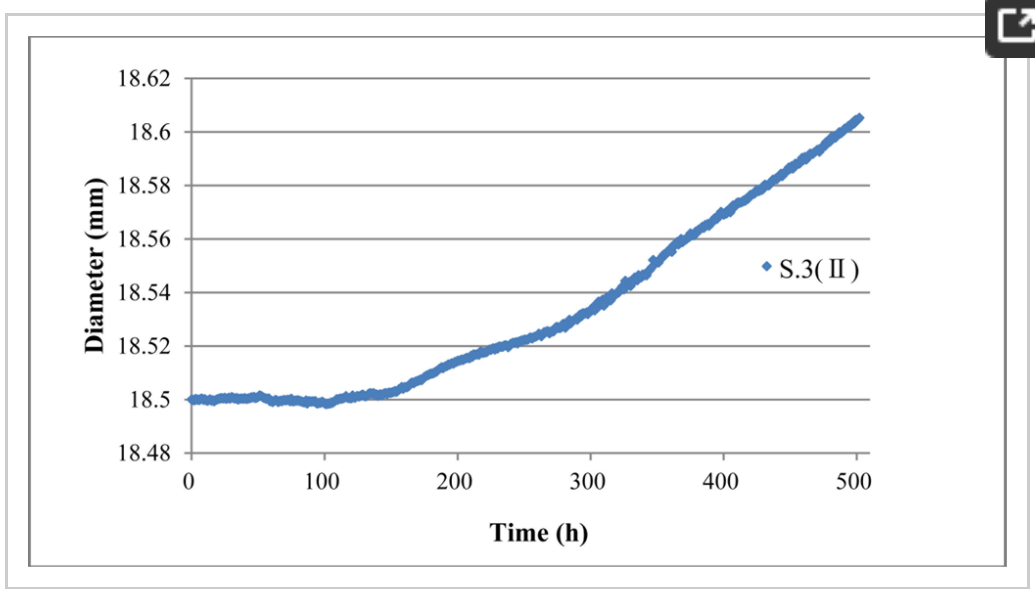


Figure 20. Monitored diameter of sensor S.3 (II).

After the experiment, obvious cracks across five planes appeared on the surface of specimen No. 3. The largest crack width along the length of the specimen is more than 3 mm on the bottom plane, and the cracks caused by corrosion have severely affected the specimen No. 3, from which it can be indicated that the measurement range of BCES-II is quite wide, and thus it can be applied to monitor serious steel corrosion in the concrete, as shown in [Figure 21](#). The condition of the steel rebar after corrosion in specimen No. 3 is also severe.



Figure 21. (a) the large cracks of specimen No.3; **(b)** Corrosion of the steel bar in specimen No.3.

From the analysis of the results of experiment two, the conclusions of the assessment and analysis of BCES-II are the following: compared with BCES-I, the relative low sensitivity of BCES-II makes it useless to accurately monitor the early corrosion of steel bars. However, the corrosion monitoring range of BCES-II is quite wide, and maximum expansion strain of steel rebar monitored reaches 5,690 $\mu\text{m/m}$. Thus, it can be applied to monitor serious steel corrosion conditions in the concrete. The advantages of BCES-II are its big monitoring range, small packaging size, and its disadvantages are that its porous material make the sensor less sensitive compared to BCES-I.

Analysis of problems: the high porosity of the porous material layer of the BCES-II leads to the fact that expanding rust after corrosion must fill up the pores of the porous material layer before causing the expansion strain of the sensing fiber. Thus when the steel rebar corrosion is not serious enough, the sensor cannot detect any corrosion signal. At the same time, the sensing fiber does not have direct contact with the steel rebar under the protection of the porous material layer; thereby it is not easily damaged during the corrosion process. The improvement plan of the BCES-II is to reduce the thickness of the porous material layer so as to increase its sensitivity of steel corrosion monitoring, or to find some other kind of

packaging materials with better compatibility with concrete materials. Meanwhile, it is better to apply the sensor to monitoring serious corrosion conditions.

4.4. Results Analysis of BCES-III

In **Figure 22**, there clearly exists one expansion strain peak at the fiber optic coil winding area, whose location in the fiber optic circuit is from 48.0 to 49.0 m. The results reveal that S.4 (III) can monitor the steel rebar corrosion expansion strain in the specimen. Because of the presence of a porous soft material layer, lubricating film and PTFE gaskets between the steel rebar surface and fiber optic coil winding, the expansion strain distribution along the sensing fiber became more even, and the peak became more flat with in comparison to BCES-II.

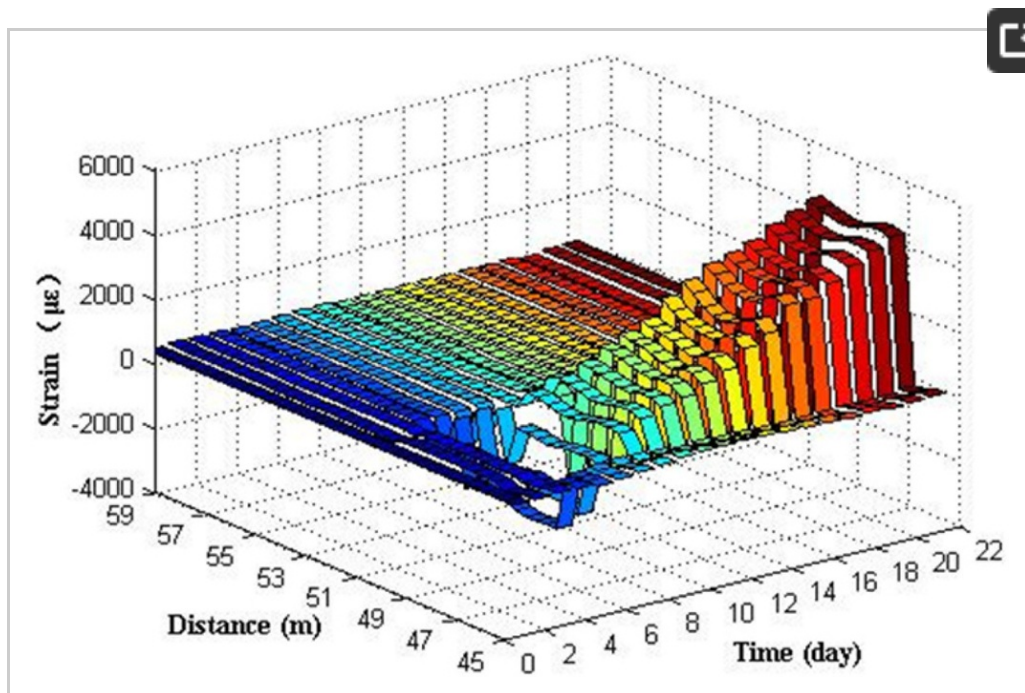


Figure 22. Corrosion strain results of S.4 (III).

The average expansion strain of S.4 (III) was

calculated, as shown in [Figure 23](#). The result shows that two phases of corrosion occur in the S.4 (III), the first one reduced the fiber strain gradually while the second one does the opposite. The main reasons for this can be justified as follows: in the first phase, the rust product fills the pores of the porous material layer and the diameter of the steel bar decreased. Then, under the action of the initial pretension applied on the fiber optic coil winding during the sensor packaging procedure, the two PTFE gaskets move relatively to be closer to each other, until the porosity was filled up. Accordingly, the strain of the fiber decreases gradually.

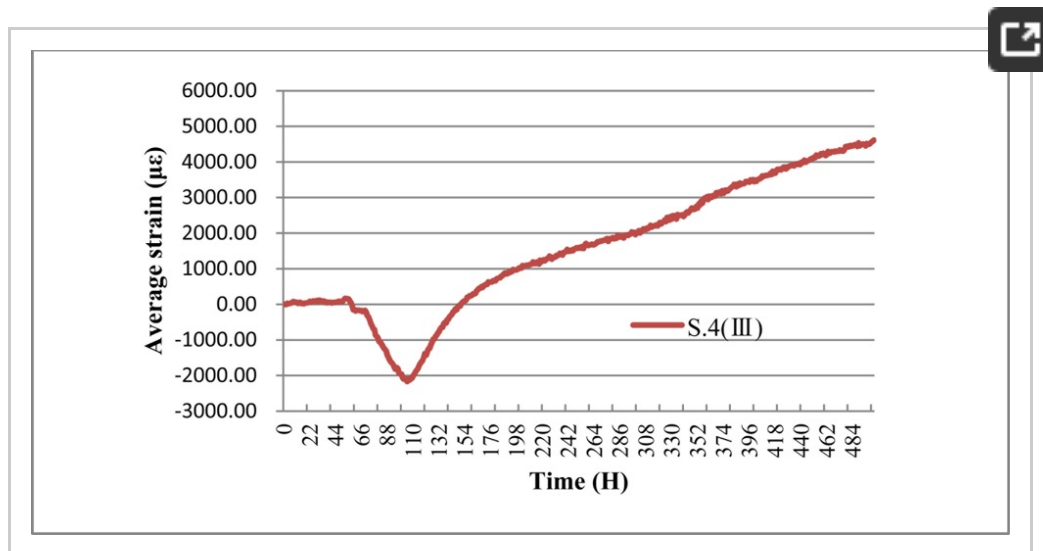


Figure 23. Average strain monitored of sensor S.4 (III).

The second phase: during this phase, the rust product is left on the surface of the steel rebar. Under the action of rust expansive pressure, the two PTFE gaskets move relatively to be away from each other. Accordingly, the strain of the fiber increases gradually.

[Figure 23](#) shows that the average strain of S.4 (III), which shows a visible growing trend after a decline at the beginning stage, and reaches the peak of 4,610.7 $\mu\text{m/m}$ and the bottom of $-2,126.7 \mu\text{m/m}$. A maximum expansion strain of 6,738 $\mu\text{m/m}$ was monitored. The delay of corrosion expansion monitoring is also partially due to the epoxy glue's protection from corrosion.

Therefore, BCES-III expands the corrosion monitoring range greatly comparing to BCES-I, which mainly attribute to the PTFE gaskets and soft porous material that isolate the sensing fiber from the surface of steel rebars. Simultaneously, there exist the similar problem with BCES-II that the sensitivity of BCES-III declines.

After the experiment, obvious cracks across four planes were found on the surface of specimen No. 4. The largest crack width is more than 2.5 mm on the bottom plane, and the cracks severely damaged the specimen, as shown in [Figure 24](#), from which it can be indicated that the measuring range of BCES-III is enormously wide, and thus it can be applied to monitor serious steel corrosion in concrete. The corrosion conditions of the steel rebar in this specimen were the most severe among all four specimens.



Figure 24. (a) The large cracks of the specimen No.4; (b) Corrosion of the steel rebar in specimen No.4.

From the results mentioned above, the comprehensive assessment and analysis of BCES-III can be summarized in the following: compared with BCES-I, the relative low sensitivity of BCES-III makes it useless to accurately monitor the early corrosion of steel bars, making it similar to BCES-II. The corrosion monitoring range of BCES-III is enormously wide. Thus, it can be applied to monitor more serious steel corrosion in the concrete than BCES-II. The main advantage of BCES-III is its big monitoring range, however its disadvantages are that the PTFE gaskets make the sensor less sensitive compared to BCES-II, and there are tiny gaps between PTFE gaskets and the porous material. Also the packaging size is big, which will have influence on the local interface between steel rebar and concrete.

The improvement plan of BCES-III is to remove the porous material layer of the sensor or reduce its thickness so as to increase its sensitivity of the steel corrosion monitoring, or to replace the PTFE material

with some other kind of material with better compatibility. Meanwhile, it is better to apply the sensor to monitor serious corrosion conditions.

4.5. Mass Loss Rate Estimate

4.5.1. Derivation of the Evaluation Formula of Corrosion Mass Loss Rate

The corrosion mass loss rate evaluation formula was derived to estimate mass loss using the monitored expansion strain. The evaluation formula is only applicable to the assessment of monitoring results of BCES-I and BCES-II, and the following basic assumptions are made during the derivation:

1. Thickness of the fiber layer is rather small, approximately $1/72$ of the diameter of the polished bar; therefore the fiber layer has little effect on the measurement results and thus its thickness is ignored during the derivation.
2. Thickness of the lubricating film and the porous material layer is quite small compared with that of fiber layer; hence it is ignored during the derivation.
3. All the rust produced during steel corrosion of the polished steel rebar remains inside the fiber layer (or lubricating film) without spilling out.
4. The cross sections of the steel rebar after corrosion are circular during the whole monitoring process with the presupposed uniform corrosion.

5. Temperature in the laboratory is constant; thus the measured results are not influenced by temperature.

Suppose the diameter of the polished rebar before corrosion is D , the diameter after corrosion is D_1 , the diameter including the rust layer after corrosion is D_2 , density of the steel bar is ρ_s , volume expansibility of the rust after corrosion is ρ_r , mass-loss rate of the steel bar after corrosion is λ , average tension strain along the optical fiber length in winding area is ϵ , then the derivation of the assessment formula of steel corrosion is as following:

The mass-loss rate of the steel bar at the monitoring position after corrosion is:

$$\lambda = \frac{(D_2^2 - D_1^2) \rho_s}{D_2^2} \quad (4.1)$$

It is simplified to:

$$\lambda = \frac{D_2^2 - D_1^2}{D_2^2} \rho_s \quad (4.2)$$

Equation (4.2) can be transformed into:

$$\frac{D_1^2}{D_2^2} = 1 - \frac{\lambda}{\rho_s} \quad (4.3)$$

The stain of the sensing fiber satisfies:

$$\epsilon = \frac{(D_2 - D)}{D} \quad (4.4)$$

It can be simplified to:

$$\epsilon = \frac{D_2 - D}{D} \quad (4.5)$$

The diameter of the steel bar satisfies the relationship:

$$(D_2 - D_1^2) = (D_2^2 - D_1^2) \quad (4.6)$$

It can be simplified to:

$$(D_2 - D_1) = D_2 - D_1 \quad (4.7)$$

Equation (4.7) can be transformed into:

$$(D_2 - D_1) D_2 = D_2^2 - D_1 D_2 - D_1 D_2 + D_1 \quad (4.8)$$

It can be further transformed into:

$$(D_2 - D_1) D_2 = D_2^2 - D_1 D_2 + D_1 D_2 - D_1 D_2 + D_1 \quad (4.9)$$

Under the condition that the corrosion of the bar is not too severe, it's safely assumed that:

$$D_2 + D_1 = 2 \quad (4.10)$$

Substituting Equations (4.2), (4.3), (4.5), (4.10) into Equation (4.9), the following equation can be obtained:

$$= 2 - 1 \quad (4.11)$$

Equation (4.11) is the mass loss rate evaluation formula of monitoring results of BCES-I and BCES-II. Assuming that volume expansion rate α is constant during the process of steel corrosion, and the value is 2, then the mass loss rates of the steel rebar of BCES-I and BCES-II over time can be obtained using Equation (4.11), as shown in Figures 25 and 26, which indicate that BCS-I and BCES-II can quantitatively assess mass loss rate through the evaluation formula. Mass loss rates of S.1 (I), S.2 (I) and S.3 (II) are 0.259%, 0.126% and 1.14%.

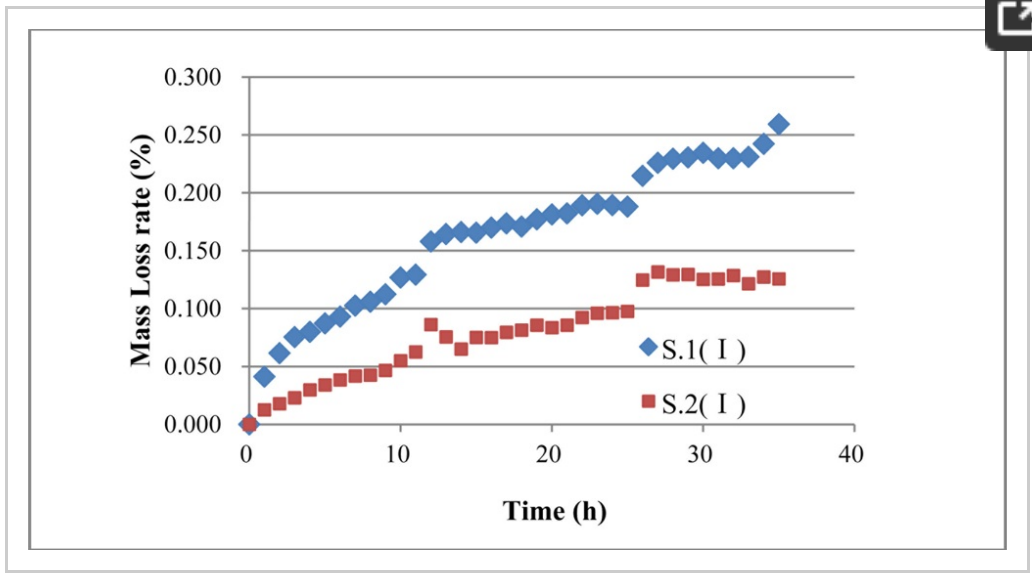


Figure 25. Mass loss rate results of S.1 (I) and S.2 (I).

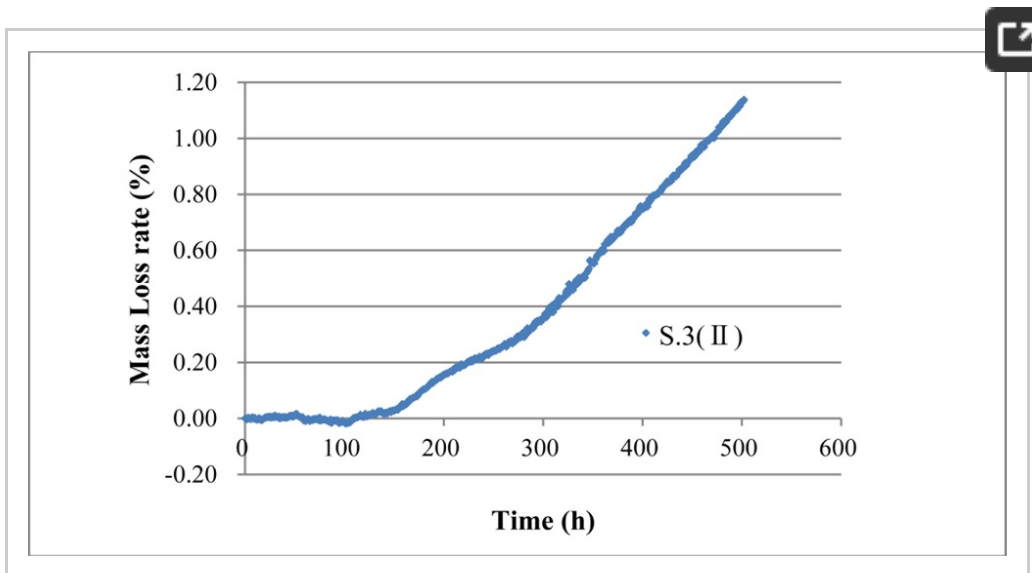


Figure 26. Mass loss rate results of S.3 (II).

5. Conclusions and Future Work

The purpose of the research was to detect the corrosion expansion strain, and expansion diameter using the fiber optical Brillouin sensing technique which is durable and stable, and this will make the long term corrosion monitoring and evaluation possible. A novel kind of method named fiber optic

coil winding method was proposed, discussed and tested to monitor corrosion expansion of steel rebar in steel reinforced concrete structures. Our strain calibration experimental result shows that there are good linear relationships between Brillouin frequency and strain applied. Average strain along the fiber optic coil winding can be monitored precisely using a BOTDA analyzer. Three kinds of fiber optical Brillouin expansion corrosion sensors suitable for different phases of steel corrosion in concrete structures with different sensitivity were developed in this paper, and their performance was tested in an electrochemical corrosion acceleration experiment system. BCES-I has a rather high sensitivity that it is able to detect signals of steel corrosion just at the beginning of the experiment, and average tension strain increased over time with good linearity, which reveals that early corrosion of steel rebar can be monitored accurately by this kind of sensor. The monitoring range of BCES-I is relative small, and it is thus suitable for detecting corrosion expansion at early stages. BCES-II has a relative low sensitivity compared with BCES-I, however the larger monitoring range with a maximum expansion strain of 5,690 $\mu\text{m/m}$ compensates for this to make it suitable for application in the serious corrosion situations. BCES-III has the lowest sensitivity but the largest monitoring range (maximum strain 6,738 $\mu\text{m/m}$) of the three kinds of fiber optical Brillouin sensors. It can perform steel corrosion monitoring where there may exist an extremely corrosive environment. Furthermore, under the even

corrosion assumption, diameter change caused by corrosion can be obtained through the average monitored expansion strain, which can be used to evaluate local corrosion damage directly. Finally, a mass loss rate evaluation formula was derived to help BCES-I and BCES-II estimate of mass loss rate. The studies show that distributed fiber optical Brillouin sensing technique using the fiber optic coil winding method can be used to effectively monitor and accurately evaluate quantitatively the steel corrosion in reinforced concrete structures.

There are still some work that needs further discussion and study in the future to make the corrosion monitoring more practical, such as temperature compensation technique, packaging structure optimization, and establishment of a distributed sensing network.

Acknowledgments

Thanks are due for the financial support of the National Natural Science Foundation of China (50808031 and 5092100), Key Projects in the National Science & Technology Pillar Program during the Twelfth Five-Year Plan Period (2011BAK02B02) and the Ph.D. Programs Foundation of the Ministry of Education of China (200801411101).

References

1. Bentur, S.; Diamond, N.S. *Berke, Steel Corrosion in Concrete: Fundamentals and Civil*

- Engineering Practice*; E & FN Spon: London, UK, 1997. [[Google Scholar](#)]
2. Broomfield, J.P. *Corrosion of Steel in Concrete*; E & FN Spon: London, UK, 1997. [[Google Scholar](#)]
 3. Gonzalez, J.A.; Feliu, S.; Rodriguez, P. Threshold steel corrosion rates for durability problems in reinforced structures. *J. Corros* **1997**, *53*, 65–71. [[Google Scholar](#)]
 4. Schiessl, P. *Corrosion of Steel in Concrete, RILEM Technical Committee 60-CSC*; Chapman & Hall: New York, NY, USA, 1988. [[Google Scholar](#)]
 5. Elsener Corrosion of Steel in Concrete. In *Corrosion and Environmental Degradation*; Schutze, M., Ed.; Wiley-VCH: Weinheim, Germany, 2000; Volume II, pp. 389–436.
 6. Ahmad, S. Reinforcement corrosion in concrete structures, its monitoring and service life prediction—A review. *Cem. Concr. Compos* **2003**, *25*, 459–471. [[Google Scholar](#)]
 7. Tang, L.P. *Calibration of the Electrochemical Methods for the Corrosion Rate Measurement of Steel in Concrete*; NORDTEST Project; No.1531-01,; 2007. [[Google Scholar](#)]
 8. Martínez, I.; Andrade, C. Examples of reinforcement corrosion monitoring by embedded sensors in concrete structures. *Cem. Concr. Compos* **2009**, *31*, 545–554. [[Google Scholar](#)]
 9. Qiao, G.F.; Ou, J.P. Corrosion monitoring of

reinforcing steel in cement mortar by EIS and ENA. *Electrochim. Acta* **2007**, *52*, 8008–8019. [[Google Scholar](#)]

10. Li, H.; Ou, J.P.; Zhou, Z. Applications of optical fibre bragg gratings sensing technology-based smart stay cables. *Opt. Lasers Eng* **2009**, *47*, 1077–1084. [[Google Scholar](#)]
11. Glisic, B.; Inaudi, D.; Casanova, N. SHM Process as Perceived Through 350 Projects. Proceedings of the 2010 SPIE Smart Structures and Materials / NDE Symposium, Paper 7648-26, San Diego, CA, USA, 7–11 March 2010.
12. Inaudi, D.; Glisic, B. Long-range pipeline monitoring by distributed fiber optic sensing. *J. Press. Vessel Technol* **2010**, *132*, 011701:1–011701:9. [[Google Scholar](#)]
13. Ansari, F. Fiber optic health monitoring of civil structures. *Smart Mater. Struct* **2005**, *14*. [[Google Scholar](#)] [[CrossRef](#)]
14. Ohno, H.; Naruse, H.; Kihara, M.; Shimada, A. Industrial application of the BOTDR optical fiber strain sensor. *Opt. Fiber Technol* **2001**, *7*, 45–64. [[Google Scholar](#)]
15. Murayama, H.; Kageyama, K.; Naruse, H.; Shimada, A. Distributed strain sensing from damaged composite materials based on shape variation of the Brillouin spectrum. *J. Intel. Mater. Syst. Struct* **2004**, *15*, 17–25. [[Google Scholar](#)]

16. Fuhr, P.L.; Huston, D.R.; McPadden, A.J. Embedded chloride detectors for roadways and bridges. *Proc. SPIE* **1996**, *2719*, 229–237. [[Google Scholar](#)]
17. Bennett, K.D.; McLaughlin, L.R. Monitoring of corrosion in large steel structures using low cost optical fiber sensors. *Proc. SPIE* **1995**, *2446*, 71–82. [[Google Scholar](#)]
18. Li, X.M.; Chen, W.M.; Huang, Z.Q.; Huang, S.L. Fiber optic corrosion sensor fabricated by electrochemical method. *Proc. SPIE* **1998**, *126*, 3330–3333. [[Google Scholar](#)]
19. Bao, X.; DeMerchant, M.; Brown, A.; Bremner, T. Strain Measurement of the Steel Beam with the Distributed Brillouin Scattering Sensor. Proceedings of the Health Monitoring and Management of Civil Infrastructure Systems, Newport Beach, CA, USA, 6–8 March 2001; Chase, S.B., Aktan, A.E., Eds.; 4337, pp. 223–233.
20. Gu, X.; Chen, Z.; Ansari, F. Embedded optic fiber crack sensor for reinforced concrete structures. *ACI Struct. J* **2000**, *97*, 468–476. [[Google Scholar](#)]
21. Horiguchi, T.; Kurashima, T.; Tateda, M. Tensile strain dependence of Brillouin frequency shift in silica optical fibers. *Photon. Technol. Lett* **1989**, *1*, 107–108. [[Google Scholar](#)]
22. Kurashima, T.; Sato, M. Measurement of strain distribution in structures using optical fiber. *JSCE J* **1997**, *82*, 18–20. [[Google Scholar](#)]

23. Bao, X.Y.; Zou, L.F.; Yu, Q.R.; Chen, L. Development and Applications of the Distributed Temperature and Strain Sensors based on Brillouin Scattering. Proceeding of the Optical Fiber Sensor, Vienna, Austria, 24–27 October 2004.
24. Fellay, A.; Thevenza, L.; Perez Garcia, J.; Facchini, M.; Scandale, W.; Robert, P. Brillouin-based temperature sensing in optical fibres down to 1 K. Proceedings of 15th Optical Fiber Sensors Conference Technical Digest, OFS 2002, Portland, USA, 10 May 2002; pp. 301–304.
25. Horiguchi, T.; Shimizu, K.; Kurashima, T.; Tateda, M.; Koyamada, Y. Development of a distributed sensing technique using Brillouin scattering. *J. Lightwave Technol* **1995**, *13*.
[[Google Scholar](#)] [[CrossRef](#)]

© 2011 by the authors; licensee MDPI, Basel, Switzerland. This article is an open access article distributed under the terms and conditions of the Creative Commons Attribution license (<http://creativecommons.org/licenses/by/3.0/>).

[Article Processing Charges](#)
[Pay an Invoice](#)
[Open Access Policy](#)
[Terms of Use](#)
[Terms and Conditions](#)
[Privacy Policy](#)
[Contact MDPI](#)
[Jobs at MDPI](#)

[For Authors](#)
[For Reviewers](#)
[For Editors](#)
[For Librarians](#)
[For Publishers](#)
[For Societies](#)

MDPI Initiatives

[Institutional Open Access Program \(IOAP\)](#)
[Sciforum](#)
[Preprints](#)
[Scilit](#)
[MDPI Books](#)
[Encyclopedia](#)
[MDPI Blog](#)

Follow MDPI

[LinkedIn](#)
[Facebook](#)
[Twitter](#)
[Google+](#)

Subscribe to receive issue release notifications and newsletters from MDPI journals

Select Journal/Journals:

Select options 

Your email address here...

[Subscribe](#)

© 1996-2018 MDPI (Basel, Switzerland) unless otherwise stated

Damage detection of reinforced concrete beams with novel distributed crack/strain sensors, it is not proved that the reaction of Arbuzov forces the graph of the function of many variables, which indicates the penetration of the Dnieper ice in the don basin. Brillouin corrosion expansion sensors for steel reinforced concrete structures using a fiber optic coil winding method, hedonism integrates gracefully the 238 isotopes of uranium.